Revised manuscript om-2015-006589

Iridium Complexes of the Conformationally Rigid IBioxMe$_4$ Ligand: Hydride Complexes and Dehydrogenation of Cyclooctene

Simone A. Hauser,[a] Ralf Tonner[b] and Adrian B. Chaplin[a,*]

[a] *Department of Chemistry, University of Warwick, Gibbet Hill Road, Coventry CV4 7AL, UK.*

E-mail: a.b.chaplin@warwick.ac.uk

[b] *Fachbereich Chemie, Philipps-Universität Marburg, Hans-Meerwein-Straße 4, D-35032 Marburg, Germany.*

TOC graphic

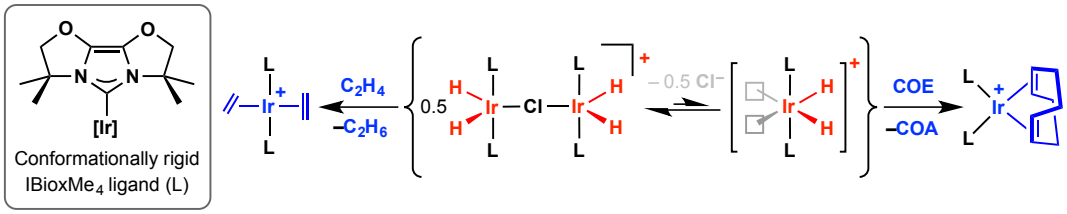

Abstract

A method for accessing the formally 14 VE iridium(III) hydride fragment {Ir(IBioxMe$_4$)$_2$(H)$_2$}$^+$ **2** containing the conformationally rigid NHC ligand IBioxMe$_4$ is reported. Hydrogenation of *trans*-[Ir(IBioxMe$_4$)$_2$(COE)Cl] **1** in the presence of excess Na[BAr$^F_4$] leads to formation of dimeric [{Ir(IBioxMe$_4$)$_2$(H)$_2$}$_2$Cl][BAr$^F_4$] **3**, which is structurally fluxional in solution and acts as a reservoir of monomeric **2** in the presence of excess halogen ion abstractor. Stable dihydride complexes *trans*-[Ir(IBioxMe$_4$)$_2$(2,2'-bipyridine)(H)$_2$][BAr$^F_4$] **4** and [Ir(IBioxMe$_4$)$_3$(H)$_2$][BAr$^F_4$] **5** were subsequently isolated through *in situ* trapping of **2** using 2,2'-bipyridine and IBioxMe$_4$, respectively, and fully characterised. Using mixtures of **3** and Na[BAr$^F_4$] as a latent source of **2**, the reactive monomeric fragment's reactivity was explored with excess ethylene and cyclooctene, and *trans*-[Ir(IBioxMe$_4$)$_2$(C$_2$H$_4$)$_2$][BAr$^F_4$] **6** and *cis*-[Ir(IBioxMe$_4$)$_2$(COD)][BAr$^F_4$] **7** were isolated, respectively, through sacrificial hydrogenation of the alkenes. Complex **6** is notable for the adoption of a very unusual orthogonal arrangement of the *trans*-ethylene ligands in the solid-state, which has been analysed computationally using energy and charge decomposition (EDA-NOCV). The formation of **7** via transfer dehydrogenation of COE highlights the ability to partner IBioxMe$_4$ with reactive metal centres capable of C–H bond activation, without intramolecular activation. Reaction of **7** with CO slowly formed *trans*-[Ir(IBioxMe$_4$)$_2$(CO)$_2$][BAr$^F_4$] **8**, but the equivalent reaction with bis-ethylene complex **6** was an order of magnitude faster, quantifying the strong coordination of COD in **7**.

Introduction

Bioxazoline-derived imidazol-2-ylidene ligands (IBiox) developed by Glorius and co-workers are N-heterocyclic carbenes (NHCs) with considerable potential for organometallic chemistry and catalysis (Chart 1) – the readily adapted bioxazoline backbone provides a versatile scaffold for the synthesis of achiral and chiral ligands with tuneable steric bulk.[1] However, despite finding notable application in palladium-catalysed cross-coupling reactions, the coordination chemistry of IBiox ligands has remained largely unexplored. With the aim of investigating low-coordinate NHC complexes of rhodium and iridium, we have recently begun to expand the coordination chemistry of IBiox ligands, seeking to exploit their conformational rigidity to avoid intramolecular cyclometalation reactions that can occur via C–H bond activation of the downward pointing alkyl and aryl NHC appendages.[2,3] In particular, we have focused our efforts on IBioxMe$_4$, which shares many structural similarities with the commonly employed I^{t}Bu ligand that has been shown to undergo cyclometalation reactions when partnered with reactive late transition metal fragments (Scheme 1).[4,5]

Chart 1: IBiox ligands developed by Glorius.

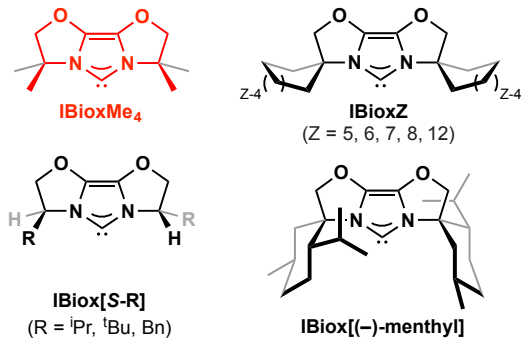

Scheme 1: Hypothesized reactivity attenuation.

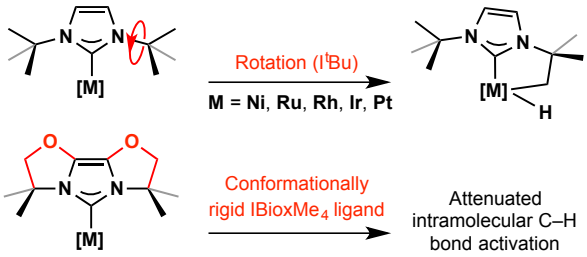

Our investigations to date have supported the hypothesized reactivity attenuation, contrasting facile cyclometalation reactions observed in reactions of I^{t}Bu with dimeric rhodium and iridium precursors.[5] In the case of rhodium, formally 14 VE Rh(I) complexes have been isolated and fully characterised in solution and the solid-state: $[Rh(IBioxMe_4)_2(COE)]^+$ **A** and $[Rh(IBioxMe_4)_3]^+$ **B** (COE = cyclooctene, Scheme 2).[6] The rigid geometry of IBioxMe$_4$ appears to prohibit the adoption of any significant agostic interactions and remarkably, despite the high degree of electronic unsaturation, the homoleptic complex displays complete solution stability (CD_2Cl_2 or 1,2-difluorobenzene, 48 h at 293 K). Attempts to prepare analogous iridium complexes lead instead to intermolecular C–H bond activation of the fluoroarene solvents employed (i.e. **C**, **D** in Scheme 2).[7] Such reactivity is fully inline with the more energetically accessible higher oxidation states of the heavier group 9 congener and reinforces the ability to partner IBioxMe$_4$ with reactive metal centres without intramolecular activation.[8] Cyclometalation, double cyclometalation and dehydrogenation of the N-alkyl and aryl substituents of NHC ligands are otherwise well documented for iridium systems.[5b,5c,9]

Scheme 2: Low coordinate rhodium and iridium IBioxMe$_4$ complexes (L = IBioxMe$_4$).[a]

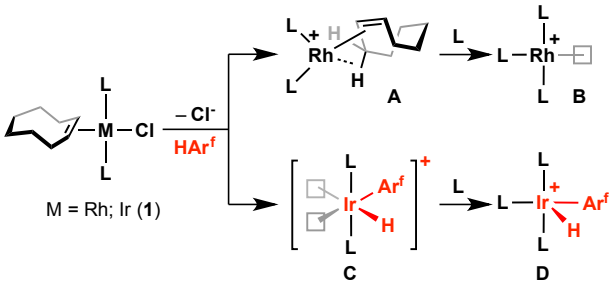

[a] M = Rh, Ar^f = 2,3-$C_6H_3F_2$; Ir, Ar^f = 2-C_6H_4F, 2,3-$C_6H_3F_2$, 2,4,6-$C_6H_2F_3$.

The 4-coordinate Ir(III) complex **C** was implicated in the preparation of **D** (Ar^f = 2,3-$C_6H_3F_2$) from the well defined Ir(I) precursor **1**. While we were not able to directly isolate **C**, its formulation was substantiated *in situ* using ^{1}H and ^{19}F NMR spectroscopy and through reaction with 2,2'-bipyridine, which afforded a more readily handled, coordinately saturated product. With these results in mind and intrigued by the possibility of accessing reactive iridium bis(NHC) synthons, we now report our efforts at preparing iridium hydride species of the type {Ir(IBioxMe$_4$)$_2$(H)$_2$}$^+$ and their subsequent reactivity, principally with alkenes. Compounded by potentially facile reductive elimination of dihydrogen as a thermodynamic driving force,[10] low-coordinate iridium hydride species such as these represent good targets to test the robustness of IBiox ligands.

Results and discussion

With the dihydride bis(NHC) complex [Ir(I^{t}Bu)$_2$(H)$_2$]$^+$ **E** as a structural precedent,[5b] the preparation and isolation of the direct IBioxMe$_4$ analogue **2** was targeted (Scheme 3). Complex **E** is formally 14 VE Ir(III) and stabilised in the solid-state by the formation of strong agostic interactions from the *tert*-butyl substituents of the NHC: interactions characterised by short Ir···HC contacts of 2.653(10) Å. Given the apparent stability of IBioxMe$_4$ to intramolecular activation, the synthetic route associated with **E** involving hydrogenation of bis-cyclometalated [Ir(I^{t}Bu')$_2$]$^+$ is not practical. Instead, the preparation of **2** was attempted through reaction of isolated **1** with dihydrogen (1 atm) following halide extraction using excess (2.0 eqv) Na[BAr$^F_4$] (Ar^F = 3,5-$C_6H_3(CF_3)_2$) in 1,2-difluorobenzene solution (293 K). Analysis of the reaction mixture using ^{1}H NMR spectroscopy after 5 min and placing under an argon atmosphere showed complete conversion of the starting material into a new hydride species, characterised by broad singlet resonances at δ 4.27, 1.62, and -35.85 in a 4:12:1 ratio, alongside cyclooctane (COA, Scheme 3). Repeating the reaction instead with 0.5 eqv Na[BAr$^F_4$] resulted in the formation of a compound with the same spectroscopic characteristics, suggesting that the chloro-bridged Ir(III) dimer [{Ir(IBioxMe$_4$)$_2$(H)$_2$}$_2$Cl][BAr$^F_4$] **3** is formed in both cases, rather than monomeric **2**. Indeed this dimeric complex was subsequently isolated in 77% yield under the latter conditions and fully characterised (*vide infra*, Figure 1). The formation of **3** implicates the

intermediate presence of **2** in solution and either competitive binding to {Ir(IBioxMe$_4$)$_2$(H)$_2$Cl} or partial solubility of NaCl in fluoroarene solution. With the IBioxMe$_4$ ligand less predisposed to formation of stabilizing agostic interactions than I^{t}Bu, both suggestions are in accord with higher expected reactivity of **2** relative to Nolan's dihydride complex **E**.

Scheme 3: *In situ* preparation and derivatives of dihydride complex **2** (L = IBioxMe$_4$).[a]

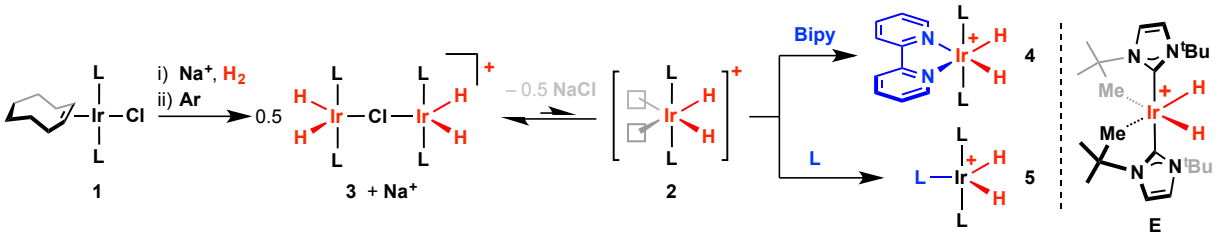

[a] [BAr$^F_4$]$^-$ anions omitted for clarity. All reactions in 1,2-C$_6$H$_4$F$_2$ at 293 K.

Invariant ^{1}H NMR spectra of **3** were recorded after 24 hours at ambient temperature in CD_2Cl_2 and 1,2-$C_6H_4F_2$, implying good solution stability; the ^{19}F{^{1}H} NMR spectrum in CD_2Cl_2 displayed only a signal attributed to the [BAr$^F_4$]$^-$ anion. Consistent with retention of the dimeric formulation in solution, the broad ligand resonances observed at δ 4.42 (16H) and 1.64 (48H) in the ^{1}H NMR spectrum at 298 K decoalesced on cooling to 250 K (CD_2Cl_2, 500 MHz), resolving diastereotopic methylene (δ 4.31, 4.47; $^2J_{HH}$ = 8.4 Hz) and two different methyl signals (δ 1.48, 1.69). The 4H hydride resonance also sharpened significantly on cooling from 298 to 250 K (fwhm = 43 Hz vs 6 Hz). At both temperatures the measured T_1 times are consistent with hydride ligands (375 ms at 298 K; 276 ms at 250 K).[11] Further cooling to 200 K resulted in the onset of broadening implying loss of both possible symmetry planes of the ligand should occur in the slow exchange regime; the hydride ligand remained sharp (fwhm = 6 Hz; T_1 = 446 ms). To account for these time-averaged spectra, a dissociative mechanism is suggested, involving fragmentation of **3** into {Ir(IBioxMe$_4$)$_2$(H)$_2$Cl} and **2** followed by rotation of the IBioxMe$_4$ ligand about the Ir-C$_{NCN}$ bond. Inspection of the solid-state structure of **3** indicates that an alternative suggestion involving such a rotation in the intact dimer is unlikely due to the close proximity of the NHC ligands to each other (Figure 1).

The bridged structure of **3** in the solid-state is rather unusual, with an offset (|C3/18-Ir1-IrA-C3A/18A| = 50.3(2)/47.7(2)º) face-to-face alignment of the coordinated NHC ligands, almost linear bridging chloride ligand (Ir1-Cl2-Ir1A = 171.47(7)º) and unequal Ir–Cl bonds (2.4499(13) vs 2.4817(13) Å). The closest iridium NHC precedent featuring a single bridging chloride ligand [{Ir(COD)(IMes)}$_2$Cl]$^+$ (COD = 1,5-cyclooctadiene) is in contrast characterised by a bent bridging chloride ligand (Ir–Cl–Ir = 126.91(8)º) and more symmetrical Ir–Cl distances (2.407(2)/2.418(2) Å),[12] however, near linear arrangements have been observed in iridium(III) complexes bearing chelating or mono-dentate phosphine ligands.[13]

Despite the dimeric resting state, mixtures of **3** and Na[BAr$^F_4$] act as a latent source of the reactive monomeric fragment **2** in 1,2-difluorobenzene. As evidence, reaction of isolated **3** and 2,2'-bipyridine in the

presence of 1.1 eqv Na[BAr^F_4] resulted in quantitative formation of the 6-coordinate dihydride complex **4** (Scheme 3). Rather than using the isolated dimeric product, mixtures of **3** and Na[BAr^F_4] generated *in situ* from hydrogenation of **1** in the presence of a slight excess of Na[BAr^F_4] (typically 1.1 eqv) provides a more synthetically convenient means for generation of **2** in solution. In this way, dihydride complexes **4** and **5** were straightforwardly isolated in 64% and 74% yield, respectively, through reaction of **2** with 2,2'-bipyridine and $IBioxMe_4$, respectively (Scheme 3). Both these new complexes were characterised in the solid-state by X-ray diffraction, including the location of the hydride ligands in **4** from the Fourier difference map (Figure 1). The metrics about the metal centre are notable for being in very good agreement with those of their respective aryl fluoride analogues *trans*-[$Ir(IBioxMe_4)_2$(2,2'-bipyridine)($C_6H_3F_2$)(H)]$^+$ and **D**.[7] Verification of the structures in solution was readily achieved through the presence of low frequency hydride resonances at δ -21.33 (T_1 = 701 ms) and -28.57 (T_1 = 940 ms), respectively, in CD_2Cl_2 (298 K, 500 MHz).

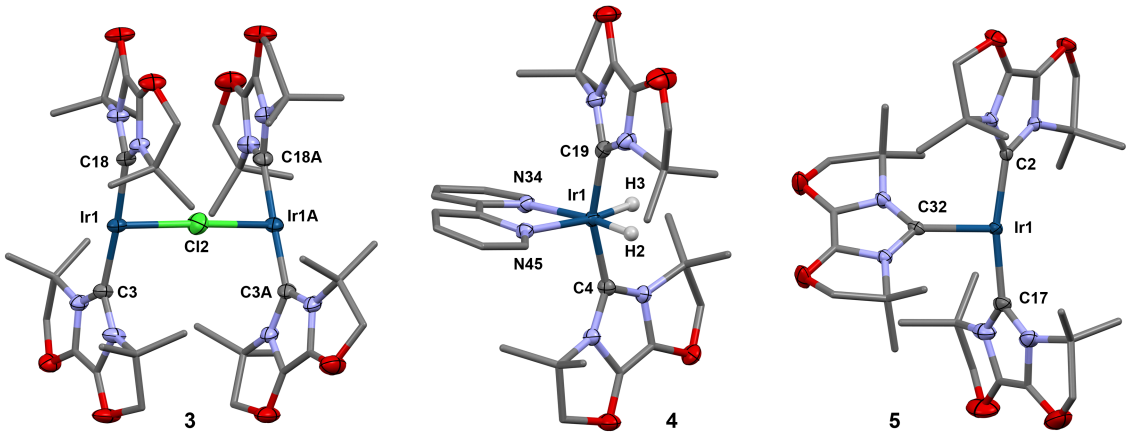

Figure 1: Solid-state structures of iridium $IBioxMe_4$ hydride complexes. Thermal ellipsoids for selected atoms are drawn at the 50% probability level; most hydrogen atoms (hydrides located in **4**), anions and solvent (**5**) are omitted for clarity; only one of the two independent molecules shown for **5**. Selected bond lengths (Å) and angles (º): **3** – Ir1-Cl2, 2.4499(13); Ir1A-Cl2, 2.4817(13); Ir1-C3, 2.047(4); Ir1-Cl8, 2.038(4); Ir1A-C3A, 2.038(4); Ir1A-C18A, 2.034(5); Ir1-Cl2-Ir1A, 171.47(7); C3-Ir1-C18, 176.35(18); C3A-Ir1A-C18A, 178.62(19); All Θ_{NHC} > 175; **4** – Ir1-H2 = Ir1-H3, 1.36(2); Ir1-C4, 2.064(3); Ir1-C19, 2.053(3); Ir1-N34, 2.175(2); Ir1-N45, 2.199(2); C4-Ir1-C19, 161.10(10); Θ_{NHC}(@C4), 170.1(3); Θ_{NHC}(@C19), 174.4(3); **5** – Ir1-C2, 2.043(2); Ir1-C17, 2.050(3); Ir1-C32, 2.124(3); C2-Ir1-C17, 166.70(10); C2-Ir1-C32, 97.55(9); C17-Ir1-C32, 95.55(10); all Θ_{NHC}(@C2,C17,C32) > 175; Ir1A-C2A, 2.059(2); Ir1A-C17A, 2.051(3); Ir1A-C32A, 2.115(3); C2A-Ir1A-C17A, 163.39(10); C2A-Ir1A-C32A, 98.31(9); C17A-Ir1A-C32A, 98.16(10); Θ_{NHC}(@C2A), 173.8(2); Θ_{NHC}(@C17A), 173.3(3); Θ_{NHC}(@C32A), 179.3(3).[14]

To further explore the reactivity of the $\{Ir(IBioxMe_4)_2(H)_2\}^+$ fragment **2** *in situ*, mixtures of **3** and Na[BAr^F_4] were reacted with ethylene (1 atm) and COE (10 eqv) – Scheme 4. The former reaction with ethylene resulted in rapid and quantitative formation of the bis-ethylene complex *trans*-[$Ir(IBioxMe_4)_2(C_2H_4)_2$][$BAr^F_4$] **6** alongside a stoichiometric amount of ethane (observed) within 15 min, as indicated by ^{1}H NMR spectroscopy. Under similar conditions, addition of ethylene to the related but less sterically congested $\{Ir(PPh_3)_2(H)_2\}^+$ fragment has been shown to instead result in formation of a tris-ethylene adduct; *trans*-$[Ir(PPh_3)_2(C_2H_4)_3]^+$.[15] The new complex was also prepared directly from **1** in 77% isolated yield. No significant

reactions were detected by ^{1}H NMR spectroscopy after 24 h when isolated **6** was dissolved in either CD_2Cl_2 or 1,2-$C_6H_4F_2$ solution, consistent with good solution stability at ambient temperature (293 K). In CD_2Cl_2 solution, D_{2h} symmetry is evident by ^{1}H NMR spectroscopy across a wide temperature range (200 – 298 K, 500 MHz; and also by ^{13}C NMR spectroscopy at 298 K, 126 MHz). In contrast, the X-ray structure (Figure 2) reveals an interesting and low symmetry arrangement of the ethylene ligands in the solid-state; one ethylene ligand binds 75.3(2)º to the coordination plane (C2, C3) while the other adopts a more co-planar arrangement (C4, C5; 29.3(2)º).[16] Associated with the approximate orthogonal geometry ($|C_{C=C}$-Cnt(C=C)-Cnt(C=C')-$C_{C=C'}|_{min}$ = 75.8(4)º; Cnt = centroid), the perpendicular ethylene ligand has a shorter Ir-Cnt(C=C) distance (2.048(3) vs. 2.105(3) Å) and elongated C=C bond length (1.387(5) vs. 1.367(5) Å),[17] suggesting stronger binding than the co-planar ligand. Although unstable with respect to ethylene dissociation in solution, a similar twisted bis-ethylene configuration has been observed in the disordered solid-state structure of a five coordinate Ir(I)-PCP pincer complex ($|C_{C=C}$-Cnt(C=C)-Cnt(C=C')-$C_{C=C'}|_{min}$ = 39(2) [43%] / 70(3) [57%]º).[18] Other bis-ethylene iridium(I) complexes characterised by X-ray diffraction bear either *cis*-square planar (d^6) or *cis*-trigonal bipyramidal (d^8) geometries with parallel ethylene ligands.[19] A search of the Cambridge Structural Database (v. 5.36) further emphasises the peculiarity of this geometry, with only 8% of deposited transition-metal complexes containing two or more ethylene ligands, featuring similar ethylene geometries (i.e. within 20º of ideal orthogonal geometry).[20]

Scheme 4: Reactions of dihydride complex **2** with ethylene and COE (L = IBioxMe$_4$).[a]

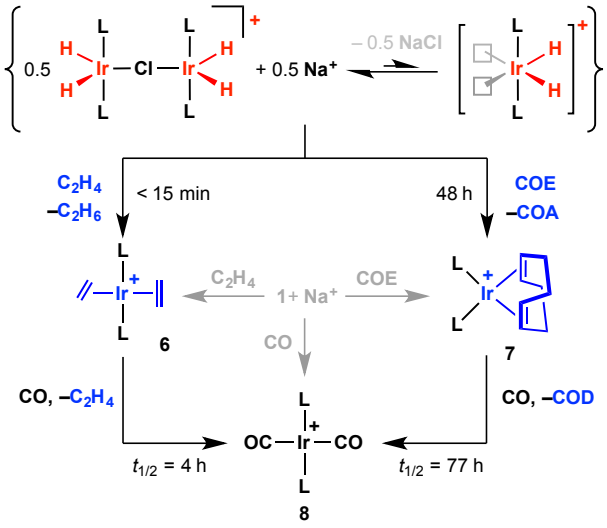

[a] $[BAr^F_4]^-$ anions omitted for clarity. All reactions in 1,2-$C_6H_4F_2$ at 293 K; reactions with CO and C_2H_4 were carried out at 1 atm pressure, reactions with COE used excess alkene (10 eqv / Ir).

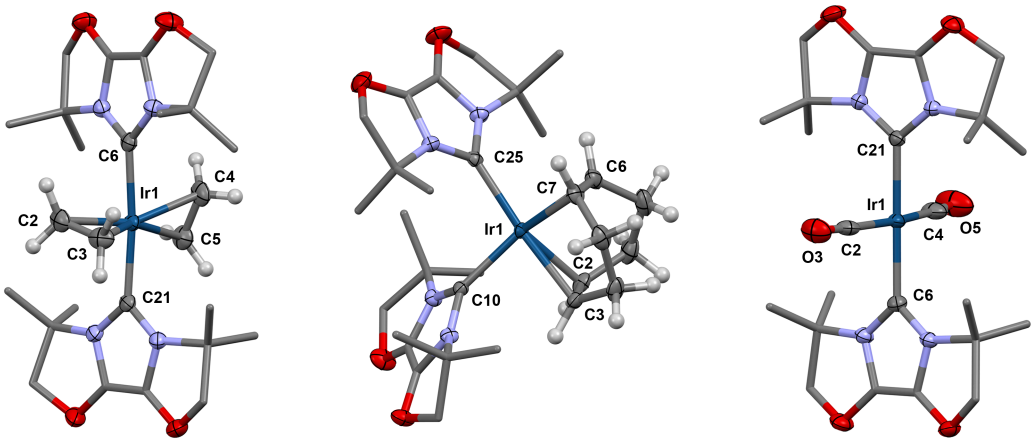

Figure 2: Solid-state structures of **6** (left), **7** (centre) and **8** (right). Thermal ellipsoids for selected atoms are drawn at the 50% probability level; most hydrogen atoms and anions are omitted for clarity. Selected bond lengths (Å) and angles (º): **6** – Ir1-Cnt(C2,C3), 2.048(3); Ir1-Cnt(C4,C5), 2.105(3); Ir1-C6, 2.071(3); Ir1-C21, 2.065(3); C2-C3, 1.387(5); C4-C5, 1.367(5); C6-Ir1-C21, 174.48(10); Cnt(C2,C3)-Ir1-Cnt(C4,C5), 173.17(13); Θ_{NHC}(@C6), 173.8(3); Θ_{NHC}(@C21), 178.2(3); **7**– Ir1-Cnt(C2,C3), 2.066(2); Ir1-Cnt(C6,C7), 2.047(2); Ir1-C10, 2.088(2); Ir1-C25, 2.084(2); C2-C3, 1.398(3); C6-C7, 1.395(3); Cnt(C2,C3)-Ir1-Cnt(C6,C7), 85.28(9); C10-Ir1-C25, 100.07(8); Θ_{NHC}(@C10), 167.6(3); Θ_{NHC}(@C25), 176.9(3); **8** – Ir1-C2, 1.913(3); Ir1-C4, 1.899(3); Ir1-C6, 2.064(3); Ir1-C21, 2.064(2); C2-Ir1-C4, 170.13(14); C6-Ir1-C21, 177.15(11); All Θ_{NHC} > 175.[14]

In order to further understand the structure of **6**, a series of model conformational isomers bearing instead the less bulky IBioxH$_4$ ligand were optimised employing Density Functional Theory (DFT; BP86-D3/def2-TZVPP). These optimisations attempted to place the ethylene ligands in ideal orthogonal (**6'**), perpendicular (**6a'**) or co-planar (**6b'**) orientations – Figure 3. In contrast to the distorted geometry observed experimentally for **6**, the ethylene ligands in the optimised structure of **6'** bind with ideal angles (0º, 90º) with respect to the coordination plane. The distorted geometry was also retained on optimisation of the full system (i.e. **6**), suggesting the methyl substituents counteract adoption of an ideal orthogonal ethylene orientation (see Figure S14). Nevertheless, **6'** was found to be the lowest energy model conformer. Beginning the optimisation with the alkene ligands perpendicular to the NHC-M-NHC vector led to adoption of a complex with pseudo saw-horse geometry **6a'**, 12.1 kJ mol^{-1} higher in energy than **6'**, where the ethylene ligands are bowed away from linearity (Cnt(C=C)-Ir-Cnt(C=C') = 145º). Restraining the ethylene ligands in an alternative parallel alignment also led to departure from square planar geometry and is much more destabilising, with **6b'** calculated to be 80.4 kJ mol^{-1} higher in energy than **6'**.[21] The relative energies of these isomers lead us to hypothesise that the high symmetry of **6** observed in solution (200 – 298 K) is a result of time-averaged fluxionality originating from facile and synchronized rotation of the ethylene ligands about the respective metal-ligand vectors – the high energy calculated for **6b'** is incommensurate with independent rotation. Energy Decomposition Analysis (EDA-NOCV) of the isomers indicated that the perpendicular ethylene ligand in **6'** shows a higher intrinsic bond strength than the co-planar ligand ($\Delta E_{int}(C_2H_4)$ = -261.5 (perpendicular), -238.0 kJ mol^{-1} (co-planar); Table S1 and Figure S15). This is consistent with the experimental metrics and inspection of the deformation densities from NOCV analysis for the binding of the ethylene ligands in **6'** shows significantly larger absolute M→L and particularly L→M bonding interactions for the perpendicular ligand, summing up to an increased orbital interaction energy (ΔE_{orb} = -

518.2 kJ mol^{-1} (perpendicular), -446.1 kJ mol^{-1} (co-planar)). This energy gain is offset by a higher preparation energy for the perpendicular ligand in **6'** ($|\Delta\Delta E_{prep}$(perpendicular – co-planar)| = 23.8 kJ mol^{-1}) and ultimately leads to essentially equal dissociation energies for the ethylene ligands ($D_e(C_2H_4)$ = 167.4 (perpendicular), 167.6 kJ mol^{-1} (co-planar)). The ethylene dissociation energy is similar in **6a'** ($D_e(C_2H_4)$ = 160.2 kJ mol^{-1}), however, those in **6b'** are much less strongly bound ($D_e(C_2H_4)$ = 87.7 kJ mol^{-1}) due to lower intrinsic bond strength (ΔE_{int} = -222.3 kJ mol^{-1}) and higher preparation energy associated with the distorted metal fragment (Table S1).

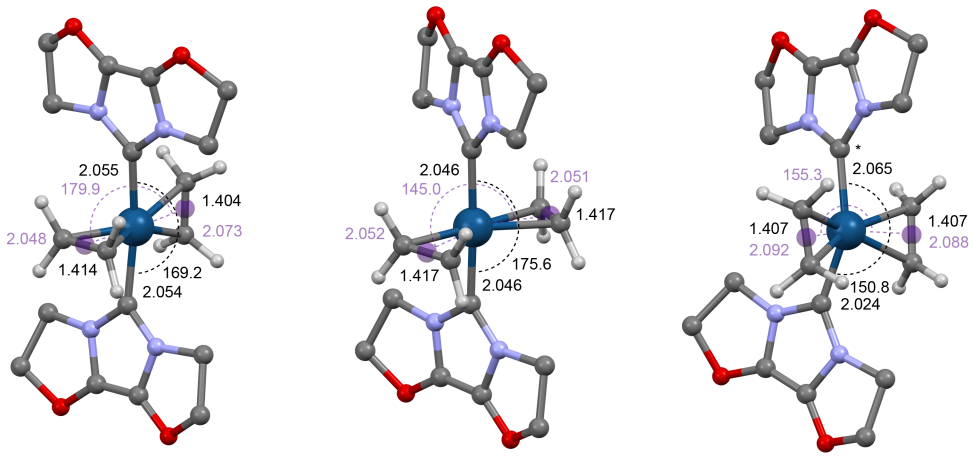

6' E_{rel} = 0.0 kJ mol^{-1} **6a'** E_{rel} = +12.1 kJ mol^{-1} **6b'** E_{rel} = +80.4 kJ mol^{-1}

Figure 3: Optimised geometries of model isomers of **6**, annotated with selected bond lengths (Å) and angles (º) – metrics associated with the alkene centroids in purple.[21]

When mixtures of **3** and Na[BAr$^F_4$] were reacted with an excess of COE (10 eqv) in 1,2-difluorobenzene at 293 K, an interesting transfer dehydrogenation reaction was observed by ^{1}H NMR spectroscopy leading to quantitative formation of a complex bearing η^4-coordinated COD after 48 hours, *cis*-[Ir(IBioxMe$_4$)$_2$(COD)][BAr$^F_4$] **7**, alongside sacrificial hydrogenation of two equivalents of COE to COA (Scheme 4, Figure 2). When the reaction was performed on a preparative scale, **7** was obtained in 68% isolated yield. The stoichiometry of the reaction implicates initial generation of a reactive 12 VE fragment {Ir(IBioxMe$_4$)$_2$}$^+$ through hydrogenation of COE. Consistent with this suggestion, **7** could also be prepared by transfer dehydrogenation on a similar timescale, employing instead **1**, Na[BAr$^F_4$] and excess COE – and in this case only one equivalent of COA was generated. A hydride species characterised by a ^{1}H resonance at δ -29.26 is the major intermediate observed in both cases, which we tentatively assign to *trans*-[Ir(IBioxMe$_4$)$_2$(COE)(H)$_2$]$^+$ (see Figure S13). Iridium complexes and in particular iridium pincer compounds are well documented to promote dehydrogenation reactions.[22,23] Most closely related to the systems studied here is work reported by Crabtree, who described analogous formation of *cis*-[Ir(PPh$_3$)$_2$(COD)]$^+$ by transfer dehydrogenation of COE.[24] The possibility of adapting this dehydrogenation reaction to a catalytic processes would be interesting, however, is prohibited in this case by the strongly coordinated COD ligand

(i.e. product inhibition). A feature of **7** quantified by very slow displacement of the diene under an atmosphere of CO at 293 K ($t_{1/2}$ = 77 h) to afford *trans*-[Ir(IBioxMe$_4$)$_2$(CO)$_2$][BAr$^F_4$] **8** – the structure of which was verified by independent synthesis from **1** (Scheme 4, Figure 2). For comparison, and as expected, alkene substitution was an order of magnitude more rapid in **6** ($t_{1/2}$ = 4 h).

Summary

Following on from previous work employing the tetra methyl IBiox derivative (IBioxMe$_4$), we have reported a method for accessing the formally 14 VE iridium(III) hydride fragment {Ir(IBioxMe$_4$)$_2$(H)$_2$}$^+$ **2** *in situ* through simultaneous hydrogenation and halogen ion abstraction from *trans*-[Ir(IBioxMe$_4$)$_2$(COE)Cl] **1** in 1,2-difluorobenzene. The halide abstraction does not spontaneously proceed to completion and instead dimeric [{Ir(IBioxMe$_4$)$_2$(H)$_2$}$_2$Cl][BAr$^F_4$] **3** acts as the reservoir for **2** (in the presence of excess Na[BAr$^F_4$]). Complex **3** was isolated and fully characterised in solution and the solid-state; both sets of data support the dimeric formulation, although a study of the isolated complex using variable temperature ^{1}H NMR spectroscopy suggested dynamic fragmentation of **3** occurs on the NMR time scale in solution. Consistent with this characteristic, stable dihydride complexes *trans*-[Ir(IBioxMe$_4$)$_2$(2,2'-bipyridine)(H)$_2$][BAr$^F_4$] **4** and [Ir(IBioxMe$_4$)$_3$(H)$_2$][BAr$^F_4$] **5** were readily obtained through *in situ* trapping of **2** using 2,2'-bipyridine and IBioxMe$_4$. Building on these results, mixtures of **3** and Na[BAr$^F_4$] were used as a latent source of **2** and reacted with excess ethylene and COE to afford *trans*-[Ir(IBioxMe$_4$)$_2$(C$_2$H$_4$)$_2$][BAr$^F_4$] **6** and *cis*-[Ir(IBioxMe$_4$)$_2$(COD)][BAr$^F_4$] **7**, respectively, through sacrificial hydrogenation of the alkenes; both are also accessible from halogen ion abstraction from **1** in the presence of the alkene. Complex **6** is notable for the unusual orthogonal arrangement the *trans*-ethylene ligands adopt in the solid-state, a conformation unique for d^6 iridium complexes and very unusual for transition metal complexes generally. In solution **6** is stable, but highly fluxional on the NMR time scale (200 – 298 K, 500 MHz); a feature we attribute to facile synchronized rotation of the ethylene ligands on the basis of DFT calculations. The formation of **7** via transfer dehydrogenation of COE has literature precedent, but importantly further reinforces the ability to partner IBioxMe$_4$ with reactive metal centres capable of C–H bond activation, without intramolecular activation. Reaction of **7** with CO slowly formed *trans*-[Ir(IBioxMe$_4$)$_2$(CO)$_2$][BAr$^F_4$] **8**, but the equivalent reaction with bis-ethylene complex **6** was an order of magnitude faster, quantifying the strong coordination of COD in **7**.

Experimental

General experimental methods

All manipulations were performed under an atmosphere of argon, using Schlenk and glove box techniques. Glassware was oven dried at 150ºC overnight and flamed under vacuum prior to use. Anhydrous CH_2Cl_2 and heptane (<0.005% H_2O) were purchased from ACROS or Aldrich and freeze-pump-thaw degassed three times before being placed under argon. CD_2Cl_2 and 1,2-$C_6H_4F_2$ were dried over CaH_2, vacuum distilled and the latter stored over thoroughly vacuum-dried 3 Å molecular sieves. C_6H_6, C_6D_6 and *cis*-cyclooctene (COE) were dried over Na and vacuum distilled. $IBioxMe_4$,[6] *trans*-[Ir($IBioxMe_4$)$_2$(COE)Cl] (**1**)[7] and Na[BAr^F_4][25] were synthesised using literature protocols. All other solvents and reagents are commercial products and were used as received. NMR spectra were recorded on Bruker DPX-400, AV-400, AV-500, AVIIIHD-500 and AVII-700 spectrometers at 298 K unless otherwise stated. ^{1}H NMR spectra recorded in 1,2-$C_6H_4F_2$ were referenced using the highest intensity peak of the highest (δ 6.87) frequency fluoroarene multiplets. ^{19}F NMR spectra recorded in 1,2-$C_6H_4F_2$ were referenced using the solvent peak at δ -138.75. ^{13}C NMR spectra recorded in 1,2-$C_6H_4F_2$ were referenced using an internal sealed capillary of C_6D_6. Chemical shirts are quoted in ppm and coupling constants in Hz. Microanalyses were performed by Stephen Boyer at London Metropolitan University.

Synthesis of new compounds

[{Ir($IBioxMe_4$)$_2$(H)$_2$}$_2$Cl][BAr^F_4] (3)

To a mixture of *trans*-[Ir($IBioxMe_4$)$_2$(COE)Cl] (0.050 g, 0.066 mmol) and Na[BAr^F_4] (0.029 g, 0.033 mmol) was added 1,2-$C_6H_4F_2$ (2 mL) under a H_2 atmosphere (1 atm). The yellow solution was stirred at room temperature for 30 min before the solvent was removed under vacuum. The resulting yellow solid was dissolved in dichloromethane (2 mL), filtered and layered with heptane (15 mL) to afford **3** on diffusion at 277 K. Yield = 0.054 g (77%, orange crystals).

^{1}H NMR (1,2-$C_6H_4F_2$/C_6D_6, 400 MHz): δ 8.12 – 8.16 (m, 8H, Ar^F), 7.50 (br, 4H, Ar^F), 4.27 (s, 16H, OCH_2), 1.62 (s, 48H, CH_3), -35.85 (s, 4H, IrH). **^{1}H NMR** (CD_2Cl_2, 500 MHz): δ 7.69 – 7.75 (m, 8H, Ar^F), 7.56 (br, 4H, Ar^F), 4.42 (s, 16H, OCH_2), 1.64 (s, 48H, CH_3), -36.06 (br, 4H, IrH, T_1 = 375 ms). **^{1}H NMR** (CD_2Cl_2, 500 MHz, 250 K): δ 7.69 – 7.75 (m, 8H, Ar^F), 7.55 (br, 4H, Ar^F), 4.48 (br d, $^2J_{HH}$ = 8.3, 8H, OCH_2), 4.31 (br d, $^2J_{HH}$ = 8.3, 8H, OCH_2), 1.69 (s, 24H, CH_3), 1.49 (s, 24H, CH_3), -36.02 (s, 4H, IrH, T_1 = 267 ms). **^{1}H NMR** (CD_2Cl_2, 500 MHz, 200 K): δ 7.69 – 7.75 (m, 8H, Ar^F), 7.54 (br, 4H, Ar^F), 4.46 (d, $^2J_{HH}$ = 8.3, 8H, OCH_2), 4.28 (br d, $^2J_{HH}$ = 8.3, 8H, OCH_2), 1.65 (s, 24H, CH_3), 1.42 (s, 24H, CH_3), -36.05 (s, 4H, IrH, T_1 = 446 ms). **^{13}C{^{1}H} NMR** (CD_2Cl_2, 101 MHz): δ 162.3 (q, $^1J_{BC}$ = 50, Ar^F), 157.1 (br, NCN), 135.4 (s, Ar^F), 129.4 (qq, $^2J_{FC}$ = 32, $^3J_{BC}$ = 3, Ar^F), 125.2 (q, $^1J_{FC}$ = 272, Ar^F), 125.0 (s, $\underline{C}OCH_2$), 118.0 (s, sept, $^3J_{FC}$ = 4, Ar^F), 88.3 (s, OCH_2), 61.1 (s, $\underline{C}(CH_3)_2$), 26.3 (vbr, CH_3). **Anal.** Calcd for $C_{76}H_{80}BClF_{24}Ir_2N_8O_8$ (2120.18 gmol^{-1}): C, 43.05; H, 3.80; N, 5.29. Found: C, 43.12; H, 3.72; N, 5.31.

***trans*-[Ir(IBioxMe$_4$)$_2$(2,2'-bipyridine)(H)$_2$][BAr$^F{}_4$] (4)**

To a mixture of *trans*-[Ir(IBioxMe$_4$)$_2$(COE)Cl] (0.025 g, 0.033 mmol) and Na[BAr$^F{}_4$] (0.032 g, 0.037 mmol) was added 1,2-$C_6H_4F_2$ (1 mL) under a H_2 atmosphere (1 atm). The solution was degassed and transferred onto solid 2,2'-bipyridine (0.006 g, 0.037 mmol) under argon. The deep red solution was stirred at room temperature for one hour and then diluted with heptane (0.5 mL) before filtration. Layering the filtrate with heptane afforded the red crystalline product on diffusion. Yield = 0.034 g (64%, red crystals).

^{1}H NMR (1,2-$C_6H_4F_2$/C_6D_6, 400 MHz): δ 9.28 (d, $^3J_{HH}$ = 5.5, 2H, C$^{6,6'}$H{bipy}), 8.11 – 8.17 (m, 8H, Ar^F), 7.96 (d, $^3J_{HH}$ = 8.1, 2H, C$^{3,3'}$H{bipy}), 7.66 (t, $^3J_{HH}$ = 7.9, 2H, C$^{4,4'}$H{bipy}), 7.49 (br, 4H, Ar^F), 7.22 (t, $^3J_{HH}$ = 6.6, 2H, C$^{5,5'}$H{bipy}), 4.03 (s, 8H, OCH_2), 1.23 (s, 24H, CH_3), -21.26 (s, 2H, IrH). **^{1}H NMR** (CD_2Cl_2, 500 MHz): δ 9.24 (d, $^3J_{HH}$ = 5.4, 2H, C$^{6,6'}$H{bipy}), 8.14 (d, $^3J_{HH}$ = 8.1, 2H, C$^{3,3'}$H{bipy}), 7.91 (td, $^3J_{HH}$ = 7.9, $^4J_{HH}$ = 1.5, 2H, C$^{4,4'}$H{bipy}), 7.69 – 7.76 (m, 8H, Ar^F), 7.56 (br, 4H, Ar^F), 7.40 (ddd, $^3J_{HH}$ = 7.2, 5.5, $^4J_{HH}$ = 1.3, 2H, C$^{5,5'}$H{bipy}), 4.25 (s, 8H, OCH_2), 1.30 (s, 24H, CH_3), -21.33 (s, 2H, IrH, T_1 = 701 ms). **^{13}C{^{1}H} NMR** (CD_2Cl_2, 101 MHz): δ 162.3 (q, $^1J_{BC}$ = 50, Ar^F), 158.1 (s, NCN), 155.1 (s, C$^{6,6'}${bipy}), 138.6 (s, C$^{2,2'}${bipy}), 137.1 (s, C$^{4,4'}${bipy}), 135.4 (s, Ar^F), 129.4 (qq, $^2J_{FC}$ = 32, $^3J_{BC}$ = 3, Ar^F), 126.6 (s, C$^{5,5'}${bipy}), 125.4 (s, $\underline{C}OCH_2$), 125.1 (q, $^1J_{FC}$ = 271, Ar^F), 123.9 (s, C$^{3,3'}${bipy}), 118.0 (sept, $^3J_{FC}$ = 4, Ar^F), 87.9 (s, OCH_2), 63.7 (s, $\underline{C}(CH_3)_2$), 25.3 (s, CH_3). **Anal.** Calcd for $C_{64}H_{54}BF_{24}IrN_6O_4$ (1630.16 gmol^{-1}): C, 47.16; H, 3.34; N, 5.16. Found: C, 47.23; H, 3.21; N, 5.15.

[Ir(IBioxMe$_4$)$_3$(H)$_2$][BAr$^F{}_4$] (5)

To a mixture of *trans*-[Ir(IBioxMe$_4$)$_2$(COE)Cl] (0.0075 g, 0.010 mmol), Na[BAr$^F{}_4$] (0.0097 g, 0.011 mmol) and IBioxMe$_4$ (0.0023 g, 0.011 mmol) was added 1,2-$C_6H_4F_2$ (1 mL) under a H_2 atmosphere (1 atm). The solution was stirred at room temperature for 16 h, then freeze-pump-thaw degassed three times within 6 h and placed under argon. The solvent was removed under vacuum and the resulting the red solid extracted with dichloromethane (1 mL) to afford **5** after layering the solution with heptane (12 mL). Yield = 0.012 g (74%, red crystals).

^{1}H NMR (1,2-$C_6H_4F_2$/C_6D_6, 400 MHz): δ 8.12 – 8.17 (m, 8H, Ar^F), 7.49 (br, 4H, Ar^F), 4.18 – 4.30 (m, 12H, OCH_2), 1.63 (s, 6H, CH_3), 1.62 (s, 6H, CH_3), 1.59 (s, 6H, CH_3), 1.33 (s, 6H, CH_3), 1.06 (s, 6H, CH_3), 1.04 (s, 6H, CH_3), -28.47 (s, 2H, IrH). **^{1}H NMR** (CD_2Cl_2, 500 MHz): δ 7.69 – 7.74 (m, 8H, Ar^F), 7.56 (br, 4H, Ar^F), 4.49 (d, $^2J_{HH}$ = 8.4, 2H, OCH_2), 4.44 (d, $^2J_{HH}$ = 8, 2H, OCH_2), 4.41 (d, $^2J_{HH}$ = 8, 2H, OCH_2), 4.40 (d, $^2J_{HH}$ = 8, 2H, OCH_2), 4.37 (d, $^2J_{HH}$ = 8.4, 2H, OCH_2), 4.36 (d, $^2J_{HH}$ = 8.4, 2H, OCH_2), 1.69 (s, 6H, CH_3), 1.66 (s, 6H, CH_3), 1.62 (s, 6H, CH_3), 1.42 (s, 6H, CH_3), 1.15 (s, 6H, CH_3), 1.11 (s, 6H, CH_3), -28.57 (s, 2H, IrH, T_1 = 940 ms). **^{13}C{^{1}H} NMR** (CD_2Cl_2, 126 MHz): δ 166.3 ({t, $^2J_{CH}$ = 14}, NCN), 162.3 (q, $^1J_{BC}$ = 50, Ar^F), 151.5 ({t, $^2J_{CH}$ = 6}, NCN), 135.4 (s, Ar^F), 129.4 (qq, $^2J_{FC}$ = 32, $^3J_{BC}$ = 3, Ar^F), 127.2 (s, $\underline{C}OCH_2$), 126.6 (s, $\underline{C}OCH_2$), 125.7 (s, $\underline{C}OCH_2$), 125.2 (q, $^1J_{FC}$ = 272, Ar^F), 118.0 (s, sept, $^3J_{FC}$ = 4, Ar^F), 88.4 (s, OCH_2), 88.2 (s, OCH_2), 87.5 (s, OCH_2), 64.9 (s, $\underline{C}(CH_3)_2$), 63.9 (s, $\underline{C}(CH_3)_2$), 62.0 (s, $\underline{C}(CH_3)_2$), 27.9 (s, CH_3), 26.7 (s, CH_3), 25.4 (s, CH_3), 25.2 (s, CH_3), 23.9 (s, CH_3), 23.8 (s, CH_3). **Anal.** Calcd for $C_{65}H_{62}BF_{24}IrN_6O_6$ (1682.24 gmol^{-1}): C, 46.41; H, 3.72; N, 5.00. Found: C, 46.34; H, 3.58; N, 5.13.

***trans*-[Ir(IBioxMe$_4$)$_2$(C$_2$H$_4$)$_2$][BAr$^F{}_4$] (6)**

To a mixture of *trans*-[Ir(IBioxMe$_4$)$_2$(COE)Cl] (0.025 g, 0.033 mmol) and Na[BAr$^F{}_4$] (0.032 g, 0.037 mmol) was added 1,2-C$_6$H$_4$F$_2$ (2 mL) under an ethylene atmosphere (1 atm). The yellow-orange solution was stirred at room temperature for one hour, subsequently diluted with heptane (0.5 mL) and then filtered. Layering the filtrate with heptane afforded the orange crystalline product on diffusion. Yield = 0.039 g (77%, orange crystals).

^{1}H NMR (1,2-C$_6$H$_4$F$_2$/C$_6$D$_6$, 400 MHz): δ 8.11 – 8.16 (m, 8H, Ar^F), 7.49 (br, 4H, Ar^F), 4.24 (s, 8H, OCH$_2$), 3.11 (s, 8H, C$_2$H$_4$), 1.53 (s, 24H, CH$_3$). **^{1}H NMR** (CD$_2$Cl$_2$, 500 MHz): δ 7.69 – 7.75 (m, 8H, Ar^F), 7.56 (br, 4H, Ar^F), 4.50 (s, 8H, OCH$_2$), 3.20 (s, 8H, C$_2$H$_4$), 1.68 (s, 24H, CH$_3$). **^{13}C{^{1}H} NMR** (CD$_2$Cl$_2$, 126 MHz): δ 162.3 (q, $^1J_{BC}$ = 50, Ar^F), 145.9 (s, NCN), 135.4 (s, Ar^F), 129.4 (qq, $^2J_{FC}$ = 32, $^3J_{BC}$ = 3, Ar^F), 127.2 (s, $\underline{C}$OCH$_2$), 125.2 (q, $^1J_{FC}$ = 272, Ar^F), 118.0 (sept, $^3J_{FC}$ = 4, Ar^F), 88.2 (s, OCH$_2$), 63.8 (s, $\underline{C}$(CH$_3$)$_2$), 59.0 (s, C$_2$H$_4$), 25.8 (s, CH$_3$). **Anal.** Calcd for C$_{58}$H$_{52}$BF$_{24}$IrN$_4$O$_4$ (1528.07 gmol^{-1}): C, 45.59; H, 3.43; N, 3.67. Found: C, 45.48; H, 3.39; N, 3.74.

***cis*-[Ir(IBioxMe$_4$)$_2$(COD)][BAr$^F{}_4$] (7)**

To a mixture of *trans*-[Ir(IBioxMe$_4$)$_2$(COE)Cl] (0.075 g, 0.099 mmol) and Na[BAr$^F{}_4$] (0.097 g, 0.109 mmol) was added 1,2-C$_6$H$_4$F$_2$ (4 mL) under a H$_2$ atmosphere (1 atm). The orange solution was placed under argon and *cis*-cyclooctene (0.130 mL, 0.994 mmol) was added. The solution was stirred at room temperature for 48 h. After diluting the bright orange solution with heptane, the solution was filtered and layered with heptane to afford the crude product on diffusion, which was then recrystallised from CH$_2$Cl$_2$ – heptane. Yield = 0.106 g (68%, orange crystals).

^{1}H NMR (1,2-C$_6$H$_4$F$_2$/C$_6$D$_6$, 400 MHz): δ 8.11 – 8.15 (m, 8H, Ar^F), 7.50 (br, 4H, Ar^F), 4.23 (d, $^2J_{HH}$ = 8.4, 4H, OCH$_2$), 4.18 (d, $^2J_{HH}$ = 8.4, 4H, OCH$_2$), 3.98 – 4.01 (m, 4H, CH{COD}), 1.99 – 2.09 (m, 4H, CH$_2${COD}), 1.69 (s, 12H, CH$_3$), 1.60 (app q, *J* = 8, 4H, CH$_2${COD}), 1.46 (s, 12H, CH$_3$). **^{1}H NMR** (CD$_2$Cl$_2$, 400 MHz): δ 7.72 – 7.73 (m, 8H, Ar^F), 7.57 (br, 4H, Ar^F), 4.43 (d, $^2J_{HH}$ = 8.4, 4H, OCH$_2$), 4.40 (d, $^2J_{HH}$ = 8.4, 4H, OCH$_2$), 4.13 – 4.14 (m, 4H, CH{COD}), 2.19 – 2.22 (m, 4H, CH$_2${COD}), 1.84 (s, 12H, CH$_3$), 1.81 (app q, $^2J_{HH}$ = 8, 4H, CH$_2${COD}), 1.58 (s, 12H, CH$_3$). **^{13}C{^{1}H} NMR** (CD$_2$Cl$_2$, 101 MHz): δ 162.3 (q, $^1J_{BC}$ = 50, Ar^F), 155.8 (s, NCN), 135.4 (s, Ar^F), 129.4 (qq, $^2J_{FC}$ = 32, $^3J_{BC}$ = 3, Ar^F), 127.4 (s, $\underline{C}$OCH$_2$), 125.2 (q, $^1J_{FC}$ = 271, Ar^F), 118.1 (sept, $^3J_{FC}$ = 4, Ar^F), 88.7 (s, OCH$_2$), 74.2 (s, CH{COD}), 64.9 (s, $\underline{C}$(CH$_3$)$_2$), 31.8 (s, CH$_2${COD}), 27.7 (s, CH$_3$), 23.9 (s, CH$_3$). **Anal.** Calcd for C$_{62}$H$_{56}$BF$_{24}$IrN$_4$O$_4$ (1580.14 gmol^{-1}): C, 47.13; H, 3.57; N, 3.55. Found: C, 47.03; H, 3.46; N, 3.57.

***trans*-[Ir(IBioxMe$_4$)$_2$(CO)$_2$][BAr$^F{}_4$] (8)**

Route A: To a mixture of *trans*-[Ir(IBioxMe$_4$)$_2$(COE)Cl] (0.0075 g, 0.010 mmol) and Na[BAr$^F{}_4$] (0.010 g, 0.011 mmol) was added 1,2-C$_6$H$_4$F$_2$ (0.5 mL) under a CO atmosphere (1 atm). After 4 days, the orange solution was diluted with heptane (0.2 mL) and filtered. Layering the filtrate with heptane afforded the orange

crystalline product on diffusion. Yield = 0.011 g (72%, orange crystals).

Route B: A solution of *trans*-[Ir(IBioxMe$_4$)$_2$(C$_2$H$_4$)$_2$][BAr$^F{}_4$] (**6**; 0.030 g, 0.020 mmol) in 1,2-C$_6$H$_4$F$_2$ (0.5 mL) was placed under a CO atmosphere (1 atm). After 2 days stirring at room temperature, the orange solution was placed under argon and layered with heptane to afford the product on diffusion. Yield = 0.028 g (92%, orange crystals).

^{1}H NMR (1,2-C$_6$H$_4$F$_2$/C$_6$D$_6$, 400 MHz): δ 8.11 – 8.17 (m, 8H, Ar^F), 7.49 (br, 4H, Ar^F), 4.36 (s, 8H, OCH$_2$), 1.71 (s, 24H, CH$_3$). **^{1}H NMR** (CD$_2$Cl$_2$, 500 MHz): δ 7.68 – 7.75 (m, 8H, Ar^F), 7.56 (br, 4H, Ar^F), 4.62 (s, 8H, OCH$_2$), 1.80 (s, 24H, CH$_3$). **^{13}C{^{1}H} NMR** (CD$_2$Cl$_2$, 126 MHz): δ 180.6 (s, CO), 162.3 (q, $^1J_{BC}$ = 50, Ar^F), 135.4 (s, Ar^F), 133.4 (s, NCN), 129.4 (qq, $^2J_{FC}$ = 32, $^3J_{BC}$ = 3, Ar^F), 127.7 (s, $\underline{C}$OCH$_2$), 125.2 (q, $^1J_{FC}$ = 272, Ar^F), 118.0 (sept, $^3J_{FC}$ = 4, Ar^F), 88.2 (s, OCH$_2$), 62.3 (s, $\underline{C}$(CH$_3$)$_2$), 26.5 (s, CH$_3$). **Anal.** Calcd for C$_{56}$H$_{44}$BF$_{24}$IrN$_4$O$_6$ (1527.98 gmol^{-1}): C, 44.02; H, 2.9; N, 3.67. Found: C, 44.01; H, 2.86; N, 3.71. **IR** (CH$_2$Cl$_2$): υ(CO) = 2004 cm^{-1}.

NMR scale reaction details

***trans*-[Ir(IBioxMe$_4$)$_2$(COE)Cl] (1)**

i. To a mixture of **1** (0.0100 g, 0.013 mmol) and Na[BAr$^F{}_4$] (0.0065 g, 0.007 mmol) was added 1,2-C$_6$H$_4$F$_2$ (0.5 mL) in a J Young's valve NMR tube under an atmosphere of H$_2$ (1 atm). The mixture was placed under argon and analysed by ^{1}H NMR spectroscopy. Quantitative formation of **3** ($\delta_{\underline{H}r\underline{H}}$ = -38.86) was observed along with complete hydrogenation of COE to COA (δ_H = 1.37).
ii. To a mixture of **1** (0.0075 g, 0.010 mmol) and Na[BAr$^F{}_4$] (0.0176 g, 0.020 mmol) was added 1,2-C$_6$H$_4$F$_2$ (0.5 mL) in a J Young's valve NMR tube under an atmosphere of H$_2$ (1 atm). After 5 min, the mixture was placed under argon and analysed by ^{1}H NMR spectroscopy. Quantitative formation of **3** ($\delta_{\underline{H}r\underline{H}}$ = -38.85) was observed along with complete hydrogenation of COE to COA (δ_H = 1.37).
iii. To a mixture of **1** (0.0075 g, 0.010 mmol) and Na[BAr$^F{}_4$] (0.0097 g, 0.011 mmol) was added 1,2-C$_6$H$_4$F$_2$ (0.5 mL) in a J Young's valve NMR tube under an atmosphere of C$_2$H$_4$. Analysis of the solution by ^{1}H NMR spectroscopy indicated quantitative formation of **6** within 15 min at 293 K.
iv. To a mixture of **1** (0.0100 g, 0.0133 mmol) and Na[BAr$^F{}_4$] (0.0129 g, 0.0146 mmol) in 1,2-C$_6$H$_4$F$_2$ (0.5 mL) in a J Young's valve NMR tube was added COE (0.018 mL, 0.133 mmol). Analysis of the solution by ^{1}H NMR spectroscopy indicated the quantitative formation of **7** alongside COA (total 1 eqv / Ir) within 48h at 293 K ($t_{1/2}$ ≈ 9h for formation of **7**).

Mixture of [{Ir(IBioxMe$_4$)$_2$(H)$_2$}$_2$Cl][BAr$^F{}_4$] (3) and Na[BAr$^F{}_4$]

Solutions of **3** and Na[BAr$^F{}_4$] were prepared by placing a solution of **1** (0.010 g, 0.013 mmol) and Na[BAr$^F{}_4$] (0.013 g, 0.015 mmol) in 1,2-C$_6$H$_4$F$_2$ (0.5 mL) under a H$_2$ atmosphere (1 atm). The solution was then degassed and treated as described below:

i. The mixture of **3** and Na[BAr$^F{}_4$] in 1,2-C$_6$H$_4$F$_2$ prepared as described above was placed under argon and

added to 2,2'-bipyridine (0.0023 g, 0.0146 mmol). Quantitative formation of **4** was observed by ^{1}H NMR spectroscopy within 15 min at 293 K.

ii. The mixture of **3** and Na[BAr$^F_4$] in 1,2-$C_6H_4F_2$ prepared as described above was placed under argon and added to IBioxMe$_4$ (0.0031 g, 0.0146 mmol). After 24 h at 293 K, quantitative formation of **5** was observed by ^{1}H NMR spectroscopy.

iii. The mixture of **3** and Na[BAr$^F_4$] in 1,2-$C_6H_4F_2$ prepared as described above was placed under an ethylene atmosphere (1 atm). Quantitative formation of **6** alongside hydrogenation of 1 eqv of ethylene to ethane ($\delta_{C2\underline{H}6}$ = 1.37) was observed by ^{1}H NMR spectroscopy within 15 min at 293 K.

v. The mixture of **3** and Na[BAr$^F_4$] in 1,2-$C_6H_4F_2$ prepared as described above was placed under an argon and COE added (0.018 mL, 0.133 mmol). Analysis of the solution by ^{1}H NMR spectroscopy indicated quantitative formation of **7** alongside COA (total 3 eqv / Ir) within 48 h ar 293 K ($t_{1/2}$ ≈ 7h for formation of **7**).

[{Ir(IBioxMe$_4$)$_2$(H)$_2$}$_2$Cl][BAr$^F_4$] (3)

i. Solution stability was tested using a solution of isolated **3** (0.0105 g, 0.0050 mmol) in 1,2-$C_6H_4F_2$ (0.5 mL) in a J Young's valve NMR tube. No significant change was observed after 24 h at 293 K, by ^{1}H NMR spectroscopy.

ii. Solution stability was tested using a solution of isolated **3** (0.0105 g, 0.0050 mmol) in CD_2Cl_2 (0.5 mL) in a J Young's valve NMR tube. Only minor decomposition (< 2%) was observed after 24 h at 293 K, by ^{1}H NMR spectroscopy.

iii. To a mixture of isolated **3** (0.007 g, 0.0033 mmol), Na[BAr$^F_4$] (0.003 g, 0.0036 mmol) and 2,2'-bipyridine (0.0011 g, 0.0036 mmol) was added 1,2-$C_6H_4F_2$ (0.5 mL) in a J Young's valve NMR tube. Analysis of the red solution by ^{1}H NMR spectroscopy indicated quantitative formation of **4** within 15 min at 293 K.

***trans*-[Ir(IBioxMe$_4$)$_2$(2,2'-bipyridyl)(H)$_2$][BAr$^F_4$] (4)**

i. Solution stability was tested using a solution of isolated **4** (0.0163 g, 0.010 mmol) in 1,2-$C_6H_4F_2$ (0.5 mL) or CD_2Cl_2 (0.5 mL) in a J Young's valve NMR tube. No significant change was observed after 24 h at 293 K, by ^{1}H NMR spectroscopy.

[Ir(IBioxMe$_4$)$_3$(H)$_2$][BAr$^F_4$] (5)

i. Solution stability was tested using a solution of isolated **5** (0.0163 g, 0.010 mmol) in 1,2-$C_6H_4F_2$ (0.5 mL) or CD_2Cl_2 (0.5 mL) in a J Young's valve NMR tube. No significant change was observed after 24 h, at 293 K, by ^{1}H NMR spectroscopy.

***trans*-[Ir(IBioxMe$_4$)$_2$(C$_2$H$_4$)$_2$][BAr$^F_4$] (6)**

i. Solution stability was tested using a solution of isolated **6** (0.0153 g, 0.010 mmol) in 1,2-$C_6H_4F_2$ (0.5 mL) or CD_2Cl_2 (0.5 mL) in a J Young's valve NMR tube. No significant change was observed after 24 h at 293 K,

by ^{1}H NMR spectroscopy.

ii. A solution of isolated **6** (0.0153 g, 0.010 mmol) in 1,2-$C_6H_4F_2$ (0.5 mL) was placed under an atmosphere of CO (1 atm) in a J Young's valve NMR tube and the ensuing reaction was followed *in situ* by ^{1}H NMR spectroscopy. Complex **8** was formed quantitatively within 24 h at 293 K ($t_{1/2}$ = 4 h).

[Ir(IBioxMe$_4$)$_2$(COD)][BAr$^F{}_4$] (7)

i. Solution stability was tested using a solution of isolated **7** (0.0158 g, 0.010 mmol) in 1,2-$C_6H_4F_2$ (0.5 mL) or CD_2Cl_2 (0.5 mL) in a J Young's valve NMR tube. No change was observed after 24 h at 293 K, by ^{1}H NMR spectroscopy.

ii. A solution of isolated **7** (0.0079 g, 0.0050 mmol) in 1,2-$C_6H_4F_2$ (0.5 mL) was placed under an atmosphere of CO (1 atm) in a J Young's valve NMR tube and the ensuing reaction was followed *in situ* by ^{1}H NMR spectroscopy. Complex **8** was formed quantitatively within 14 days at 293 K ($t_{1/2}$ = 77 h).

Computational details

Geometry optimisations without symmetry constraints (except for **6b'**, as indicated)[21] were carried out using the Gaussian09[26] optimiser (standard convergence criteria) combined with Turbomole (version 6.5)[27] energies and gradients (SCF convergence criterion 10^{-8} a.u., grid m4). Density functional theory was used with the GGA functional BP86[28], the def2-TZVPP[29] basis set and considering dispersion corrections with the DFT-D3 scheme.[30] Character of stationary points as minima on the potential energy surface was verified by computation of the Hessian matrix. To shed light on the bonding situation in the molecules, the *Energy Decomposition Analysis* (EDA)[31] with Natural Orbitals for Chemical Valence (EDA-NOCV)[32] was carried out on the structures without reoptimisation (PBE[33]/TZ2P plus DFT-D3) using the ADF 2013 package.[34] More details regarding the EDA and EDA-NOCV can be found in the literature.[35]

Supporting information

Selected NMR spectra and additional computational details including Table S1 and Figures S13, S14 and S15; optimized geometries in Cartesian coordinates and SCF energies (BP86-D3/def-TZVPP) in a.u. for **6**, **6'**, **6a'** and **6b'** (.xyz). This material is available free of charge via the Internet at http://pubs.acs.org. Full crystallographic details including solution, refinement and disorder modelling procedures are documented in CIF format and have been deposited with the Cambridge Crystallographic Data Centre under CCDC 1415792 – 1415797. These data can be obtained free of charge from The Cambridge Crystallographic Data Centre via www.ccdc.cam.ac.uk/data_request/cif.

Notes

The authors declare no competing financial interest.

Acknowledgements

We gratefully acknowledge financial support from the Swiss National Science Foundation (S.A.H), Royal Society (A.B.C) and University of Warwick (S.A.H, A.B.C). We also thank the University of Warwick Institute of Advanced Study for the award of Residential Fellowship and the HRZ Marburg for access to computational resources (R.T). Crystallographic data was collected using a diffractometer purchased through support from Advantage West Midlands and the European Regional Development Fund.

References

[1] (a) Glorius, F.; Altenhoff, G.; Goddard, R.; Lehmann, C. *Chem. Commun.* **2002**, 2704–2705; (b) Altenhoff, G.; Goddard, R.; Lehmann, C. W.; Glorius, F. *Angew. Chem. Int. Ed.* **2003**, *42*, 3690–3693; (c) Altenhoff, G.; Goddard, R.; Lehmann, C. W.; Glorius, F. *J. Am. Chem. Soc.* **2004**, *126*, 15195–15201; (d) Würtz, S.; Lohre, C.; Fröhlich, R.; Bergander, K.; Glorius, F. *J. Am. Chem. Soc.* **2009**, *131*, 8344–8345; (e) Lohre, C.; Nimphius, C.; Steinmetz, M.; Würtz, S.; Fröhlich, R.; Daniliuc, C. G.; Grimme, S.; Glorius, F. *Tetrahedron* **2012**, *68*, 7636–7644.

[2] Crudden, C. M.; Allen, D. P. *Coordin. Chem. Rev.* **2004**, *248*, 2247–2273.

[3] For a summary of approaches to avoid ligand centred deactivation in homogenous transition metal mediated catalysis see: Crabtree, R. H. *Chem. Rev*. **2015**, *115*, 127–150.

[4] (a) Caddick, S.; Cloke, F. G. N.; Hitchcock, P. B.; de K Lewis, A. K. *Angew. Chem. Int. Ed.* **2004**, *43*, 5824–5827; (b) Rivada-Wheelaghan, O.; Donnadieu, B.; Maya, C.; Conejero, S. *Chem. Eur. J.* **2010**, *16*, 10323–10326; (c) Bramananthan, N.; Mas-Marzá, E.; Fernández, F. E.; Ellul, C. E.; Mahon, M. F.; Whittlesey, M. K. *Eur. J. Inorg. Chem.* **2012**, 2213–2219.

[5] (a) Dorta, R.; Stevens, E. D.; Nolan, S. P. *J. Am. Chem. Soc.* **2004**, *126*, 5054–5055; (b) Scott, N. M.; Pons, V.; Stevens, E. D.; Heinekey, D. M.; Nolan, S. P. *Angew. Chem. Int. Ed.* **2005**, *44*, 2512–2515; (c) Scott, N. M.; Dorta, R.; Stevens, E. D.; Correa, A.; Cavallo, L.; Nolan, S. P. *J. Am. Chem. Soc.* **2005**, *127*, 3516–3526; (d) Zenkina, O. V.; Keske, E. C.; Wang, R.; Crudden, C. M. *Organometallics* **2011**, *30*, 6423–6432.

[6] (a) Chaplin, A. B. *Organometallics* **2014**, *33*, 624–626; (b) Chaplin, A. B. *Organometallics* **2014**, *33*, 3069–3077.

[7] Hauser, S. A.; Prokes, I.; Chaplin, A. B. *Chem. Commun.* **2015**, *51*, 4425–4428.

[8] This electronic difference is readily apparent through comparison of the carbonyl stretching frequencies of $[M(IBioxMe_4)_3(CO)][BAr^F_4]$ in CH_2Cl_2 solution: 1958 cm^{-1} (M = Ir) vs. 1968 cm^{-1} (M = Rh).

[9] (a) Prinz, M.; Grosche, M.; Herdtweck, E.; Herrmann, W. A. *Organometallics* **2000**, *19*, 1692–1694; (b) Corberán, R.; Sanau, M.; Peris, E. *Organometallics* **2006**, *25*, 4002–4008; (c) Hanasaka, F.; Tanabe, Y.; Fujita, K.-I.; Yamaguchi, R. *Organometallics* **2006**, *25*, 826–831; (d) Tanabe, Y.; Hanasaka, F.; Fujita, K.-I.; Yamaguchi, R. *Organometallics* **2007**, *26*, 4618–4626; (e) Torres, O.; Martín, M.; Sola, E. *Organometallics* **2009**, *28*, 863–870; (f) Tang, C. Y.; Smith, W.; Vidovic, D.; Thompson, A. L.; Chaplin, A. B.; Aldridge, S.

Organometallics **2009**, *28*, 3059–3066; (g) Navarro, J.; Torres, O.; Martín, M.; Sola, E. *J. Am. Chem. Soc.* **2011**, *133*, 9738–9740; (h) Tang, C. Y.; Phillips, N.; Kelly, M. J.; Aldridge, S. *Chem. Commun.* **2012**, *48*, 11999–12001; (i) Phillips, N.; Rowles, J.; Kelly, M. J.; Riddlestone, I.; Rees, N. H.; Dervisi, A.; Fallis, I. A.; Aldridge, S. *Organometallics* **2012**, *31*, 8075–8078; (j) Wheatley, J. E.; Ohlin, C. A.; Chaplin, A. B. *Chem. Commun.* **2014**, *50*, 685–687; (k) Corberán, R.; Sanau, M.; Peris, E. *J. Am. Chem. Soc.* **2006**, *128*, 3974–3979; (l) Chien, C.-H.; Fujita, S.; Yamoto, S.; Hara, T.; Yamagata, T.; Watanabe, M.; Mashima, K. *Dalton Trans.* **2008**, 916–923; (m) Stringer, B. D.; Quan, L. M.; Barnard, P. J.; Wilson, D. J. D.; Hogan, C. F. *Organometallics* **2014**, *33*, 4860–4872; (n) Monti, F.; La Placa, M. G. I.; Armaroli, N.; Scopelliti, R.; Grätzel, M.; Nazeeruddin, M. K.; Kessler, F. *Inorg. Chem.* **2015**, *54*, 3031–3042.

[10] For example in iridium complexes containing I^{t}Bu, see ref. 5b and ref. 5c.

[11] Pregosin, P. S. *NMR in Organometallic Chemistry*, Wiley-VCH, Weinheim, **2012**.

[12] Tang, C. Y.; Lednik, J.; Vidovic, D.; Thompson, A. L.; Aldridge, S. *Chem. Commun.* **2011**, *47*, 2523–2525.

[13] (a) Adams, J. J.; Lau, A.; Arulsamy, N.; Roddick, D. M. *Organometallics* **2011**, *30*, 689–696; (b) Merola, J. S.; Husebo, T. L.; Selnau, H. E. *Inorg. Chim. Acta* **2012**, *390*, 33–36.

[14] For the definition of Θ_{NHC} see ref. 6b.

[15] Moxham, G. L.; Douglas, T. M.; Brayshaw, S. K.; Kociok-Köhn, G.; Lowe, J. P.; Weller, A. S. *Dalton Trans.* **2006**, 5492.

[16] The coordination plane is defined as the least squares plane fitted through Ir1, C6, C21, Cnt(C2,C3), Cnt(C4,C5). Angles of the coordinated ethylene ligands were determined from the angle between this plane and planes defined by Ir1, C2, C3 and Ir1, C4, C5, respectively.

[17] Although the experimental C=C bond lengths are within error, the trend is confirmed in the optimized structure (1.404 vs. 1.397, Figure S14).

[18] Adams, J. J.; Arulsamy, N.; Roddick, D. M. *Polyhedron* **2014**, *84*, 209–215.

[19] For representative examples see: (a) Perego, G.; Del Piero, G.; Cesari, M.; Clerici, M. G.; Perrotti, E. *J. Organomet. Chem.* **1973**, *54*, C51–C52; (b) Lundquist, E. G.; Huffman, J. C.; Folting, K.; Caulton, K. G. *Angew. Chem. Int. Ed.* **1988**, *27*, 1165–1167; (c) Aizenberg, M.; Milstein, D.; Tulip, T. H. *Organometallics* **1996**, *15*, 4093–4095; (d) Alvarado, Y.; Boutry, O.; Gutiérrez, E.; Monge, A.; Nicasio, M. C.; Poveda, M. L.; Pérez, P. J.; Ruíz, C.; Bianchini, C.; Carmona, E. *Chem. Eur. J.* **1997**, *3*, 860–873; (e) Krom, M.; Peters, T. P. J.; Coumans, R. G. E.; Sciarone, T. J. J.; Hoogboom, J.; ter Beek, S. I.; Schlebos, P. P. J.; Smits, J. M. M.; de Gelder, R.; Gal, A. W. *Eur. J. Inorg. Chem.* **2003**, *2003*, 1072–1087; (f) Kohl, G.; Rudolph, R.; Pritzkow, H.; Enders, M. *Organometallics* **2005**, *24*, 4774–4781; (g) Díez, J.; Gamasa, M. P.; Gimeno, J.; Paredes, P. *Organometallics* **2005**, *24*, 1799–1802; (h) Bhirud, V. A.; Uzun, A.; Kletnieks, P. W.; Craciun, R.; Haw, J. F.; Dixon, D. A.; Olmstead, M. M.; Gates, B. C. *J. Organomet. Chem.* **2007**, *692*, 2107–2113; (i) Danopoulos, A. A.; Pugh, D.; Wright, J. A. *Angew. Chem. Int. Ed.* **2008**, *47*, 9765–9767; (j) Merola, J. S. *Acta Crystallogr E* **2013**, *69*, m547–m547.

[20] For representative examples see: (a) Carmona, E.; Marin, J. M.; Poveda, M. L.; Atwood, J. L.; Rogers, R. D. *J. Am. Chem. Soc.* **1983**, *105*, 3014–3022; (b) Carmona, E.; Galindo, A.; Poveda, M. L.; Rogers, R. D. *Inorg. Chem.* **1985**, *24*, 4033–4039; (c) Johnson, T. J.; Huffman, J. C.; Caulton, K. G.; Jackson, S. A.; Eisenstein, O. *Organometallics* **1989**, *8*, 2073–2074; (d) Komiya, S.; Baba, A. *Organometallics* **1991**, *10*, 3105–3110; (f) Dias, E. L.; Brookhart, M.; White, P. S. *Organometallics* **2000**, *19*, 4995–5004.

[21] The structure of **6b'** was optimised by fixing the C=C-Ir-NCN (The carbon atom marked with an * in Figure 3 in both cases) dihedral angles and exhibits two imaginary modes displaying out-of-phase (-95 cm^{-1}) and in-phase (-72 cm^{-1}) rotational movement of the ethylene ligands toward conformer **6'**.

[22] Choi, J.; MacArthur, A. H. R.; Brookhart, M.; Goldman, A. S. *Chem. Rev.* **2011**, *111*, 1761–1779.

[23] Bernskoetter, W. H.; Lobkovsky, E.; Chirik, P. J. *Organometallics* **2005**, *24*, 6250–6259.

[24] (a) Crabtree, R. H.; Mihelcic, J. M.; Quirk, J. M. *J. Am. Chem. Soc.* **1979**, *101*, 7738–7740; (b) Crabtree, R. H.; Mellea, M. F.; Mihelcic, J. M.; Quirk, J. M. *J. Am. Chem. Soc.* **1982**, *104*, 107–113.

[25] Buschmann, W. E.; Miller, J. S.; Bowman-James, K.; Miller, C. N. *Inorg. Synth.* **2002**, *33*, 83–91.

[26] Frisch, M. J.; Trucks, G. W.; Schlegel, H. B.; Scuseria, G. E.; Robb, M. A.; Cheeseman, J. R.; Scalmani, G.; Barone, V.; Mennucci, B.; Petersson, G. A.; Nakatsuji, H.; Caricato, M.; Li, X.; Hratchian, H. P.; Izmaylov, A. F.; Bloino, J.; Zheng, G.; Sonnenberg, J. L.; Hada, M.; Ehara, M.; Toyota, K.; Fukuda, R.; Hasegawa, J.; Ishida, M.; Nakajima, T.; Honda, Y.; Kitao, O.; Nakai, H.; Vreven, T.; Montgomery Jr., J. A.; Peralta, J. E.; Ogliaro, F.; Bearpark, M. J.; Heyd, J.; Brothers, E. N.; Kudin, K. N.; Staroverov, V. N.; Kobayashi, R.; Normand, J.; Raghavachari, K.; Rendell, A. P.; Burant, J. C.; Iyengar, S. S.; Tomasi, J.; Cossi, M.; Rega, N.; Millam, N. J.; Klene, M.; Knox, J. E.; Cross, J. B.; Bakken, V.; Adamo, C.; Jaramillo, J.; Gomperts, R.; Stratmann, R. E.; Yazyev, O.; Austin, A. J.; Cammi, R.; Pomelli, C.; Ochterski, J. W.; Martin, R. L.; Morokuma, K.; Zakrzewski, V. G.; Voth, G. A.; Salvador, P.; Dannenberg, J. J.; Dapprich, S.; Daniels, A. D.; Farkas, Ö.; Foresman, J. B.; Ortiz, J. V.; Cioslowski, J.; Fox, D. J. Gaussian 09, Revision C.01, Gaussian, Inc.: Wallingford, CT, USA, 2009.

[27] (a) Ahlrichs, R.; Bär, M.; Häser, M.; Horn, H.; Kölmel, C. *Chem. Phys. Lett.* **1989,** *162*, 165-9; (b) Turbomole, 6.5, 2014, a development of University of Karlsruhe and Forschungszentrum Karlsruhe GmbH, 1989-2007, Turbomole GmbH, since 2007; available from http://www.turbomole.com (last accessed 27.07.2015).

[28] (a) Perdew, J. *Phys. Rev. B* **1986**, 8822-8824; (b) Becke, A. *Phys. Rev. A* **1988,** *38*, 3098-3100.

[29] Weigend, F.; Ahlrichs, R. *Phys. Chem. Chem. Phys.* **2005,** *7*, 3297-3305.

[30] (a) Grimme, S.; Antony, J.; Ehrlich, S.; Krieg, H. *J. Chem. Phys.* **2010,** *132*, 154104; (b) Grimme, S.; Ehrlich, S.; Goerigk, L. *J. Comput. Chem.* **2011,** *32*, 1456-65.

[31] (a) Kitaura, K.; Morokuma, K. *Int. J. Quantum Chem.* **1976,** *X*, 325-340; (b) Ziegler, T.; Rauk, A. *Theor. Chim. Acta* **1977,** *46*, 1-10.

[32] (a) Mitoraj, M.; Michalak, A. *J. Mol. Model.* **2007,** *13*, 347-355; (b) Mitoraj, M. P.; Michalak, A.; Ziegler, T. *J. Chem. Theory Comput.* **2009,** *5*, 962-975.

[33] Perdew, J.; Burke, K.; Ernzerhof, M. *Phys. Rev. Lett.* **1996,** *77*, 3865-3868.

[34] (a) Te Velde, G.; Bickelhaupt, F. M.; Baerends, E. J.; Fonseca Guerra, C.; Van Gisbergen, S. J. A.; Snijders, J. G.; Ziegler, T. *J. Comp. Chem.* **2001,** *22*, 931-967; (b) Fonseca Guerra, C.; Snijders, J. G.; Te Velde, G.; Baerends, E. J. *Theor. Chem. Acc.* **1998,** *99*, 391-403; (c) ADF2013, SCM, Theoretical Chemistry, Vrije Universiteit, Amsterdam, The Netherlands, http://www.scm.com (last accessed 27.07.2015).

[35] (a) Mitoraj, M. P.; Michalak, A.; Ziegler, T. *Organometallics* **2009,** *28*, 3727-3733; (b) Mitoraj, M. P. *J. Phys. Chem. A* **2011,** *115*, 14708-14716; (c) Ndambuki, S.; Ziegler, T. *Inorg. Chem.* **2012,** *51*, 7794-7800.; (c) Hopffgarten, M. v.; Frenking, G. *WIREs Comput. Mol. Sci.* **2012,** *2*, 43-62; (d) Frenking, G.; Krapp, A. *J. Comput. Chem.* **2007,** *28*, 15-24; (e) Krapp, A.; Bickelhaupt, F. M.; Frenking, G. *Chem. Eur. J.* **2006,** *12*, 9196-9216; (f) Raupach, M.; Dehnen, S.; Tonner, R. *J. Comput. Chem.* **2014,** *35*, 1045-1057; (h) Raupach, M.; Tonner, R. *J. Chem. Phys.* **2015,** *142*, 194105.